

Adaptive Anti-swing Control for Clasp Operations in Quadrotors with Cable-suspended Payload

Swati Dantu, Rishabh Dev Yadav, Ananth Rachakonda, Spandan Roy, and Simone Baldi

Abstract—Crucial phases in aerial transportation and delivery of suspended payloads are the clasp and unclasp of the payload to the cable. During these phases, along with the uncertainties in the quadrotor and in the environment, the inevitable payload swings induced by the human interaction or by other external interaction will create additional state-dependent uncertainties; such uncertainties pose a significant challenge in terms of control. If they continue unabated, these uncertainties can cause safety hazard for the quadrotor, the payload and, most importantly, for the human operating the clasp/unclasp tasks. As the state-of-the-art adaptive controllers cannot tackle such uncertainties or considers them as bounded terms, this paper presents an adaptive anti-swing controller where all uncertainties are taken in a state-dependent form. This choice is made to better capture uncertain clasp and unclasp operations of the suspended payload. The closed-loop stability is studied analytically and the real-time experiments confirm significant performance improvements for the proposed scheme over the state of the art.

I. INTRODUCTION

Several civilian and military applications involving payload delivery with aerial quadrotor or quadrotor-like vehicles have been proposed and studied in recent years [1]–[3]. Of the two most typical modes of aerial payload transportation, cable-suspended (cf. [4]–[7]) and fixed gripper-based (cf. [8]–[11]), the former is usually preferred owing to its flexibility to carry payloads with different sizes without compromising the agility of the quadrotor. Crucial operational phases in the cable-suspended mode are the clasp and unclasp of the payload, typically involving interaction with a human operator itself (cf. Fig. 1). To ensure safe operations for humans, it is imperative that the quadrotor has the ability to stabilise itself against disturbances induced due to the swing in the cable.

Unfortunately, it is well known in the literature that it is a challenging problem to control such a system amid uncertainties (parametric, external wind, rotor downwash etc.), as the swing angles introduce additional unactuated degrees-of-freedom to an inherently underactuated quadrotor system. Several literature simplifies such complexity

This work was supported in part by “Aerial Manipulation” under IHFC grand project (GP/2021/DA/032), India, in part by ‘UASAT’ project sponsored by MeitY, India and in part by the National Key R&D Program of China grant 2022YFE0198700, and the Natural Science Foundation of China grants 62150610499 and 62073074.

S. Dantu, R. D. Yadav, A. Rachakonda and S. Roy are with Robotics Research Center, International Institute of Information Technology Hyderabad (IIIT-H), Hyderabad, India (e-mail: {swati.dantu, rishabhdev.yadav, ananth.rachakonda}@research.iiit.ac.in, spandan.roy@iiit.ac.in)

S. Baldi is with the School of Mathematics, Southeast University, Nanjing, China (e-mail: s.baldi@tudelft.nl).

The first three authors contributed equally.

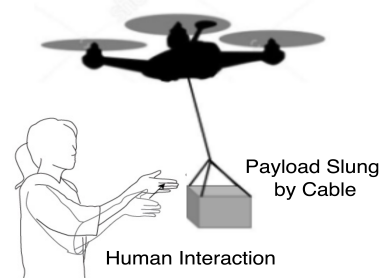


Fig. 1: Illustration of human interaction during clasp/unclasp operations in a quadrotor with cable-suspended payload.

by considering only one planar swing angle (cf. [12]–[15] and references therein); however, in the case of payload transportation, it is more realistic to consider both planar swing angles, (cf. Fig. 2). Although, adaptive controllers have been proposed considering two swing angles ([6], [16]–[18]), it is worth noticing that these works cannot tackle state-dependent unknown dynamics that are peculiar to the quadrotor case. Examples of state-dependent uncertainties include: imprecise parametric knowledge of (low velocity) drag forces, rotor downwash, coupling forces generated by the payload swing (cf. Remark 2 later). Left unattended, these unmodelled forces can create drift/ unwanted motion to the quadrotor (cf. the experimental results in Sect. IV), leading to potential hazards for the quadrotor, the payload and, most importantly, the human operating the clasp/unclasp tasks. Precise modelling of these forces is very difficult as they are sometimes dominated by the shape and size of the payload itself (e.g., rotor downwash [17], [18]).

It is evident from the above discussion that, for a safer human-quadrotor interaction, *a controller must be designed to stabilize the payload swing angles in the presence of unknown state-dependent uncertainties*. The proposed work solves this largely unsolved control in the existing literature. The highlights of this work are:

- adaptive anti-swing control with estimation of unknown state-dependent dynamics and external disturbances without their a priori knowledge;
- closed-loop stability analysis via the Lyapunov approach;
- real-time experimental results in comparison to the state-of-the-art, showing significantly improved system stabilization against external disturbances induced by the payload swing.

This work extends previous quadrotor research by some of the authors, since [19], [20] did not consider explicitly any

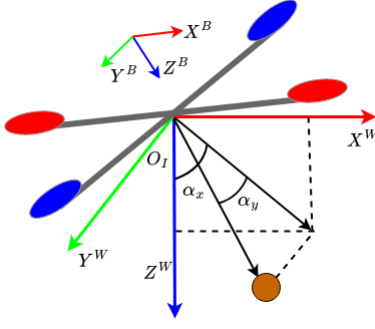


Fig. 2: Illustration of a quadrotor system with suspended payload.

TABLE I: Nomenclature

$[X^B \ Y^B \ Z^B]$	Quadrotor body-fixed coordinate frame
$[X^W \ Y^W \ Z^W]$	Earth-fixed coordinate frame
$[x \ y \ z]$	Quadrotor position in Earth-fixed coordinate frame
$[\phi \ \theta \ \psi]$	Quadrotor roll, pitch and yaw angles
α_x	Payload projection angles in $X^W Z^W$ plane
α_y	Payload projection angle in $Y^W Z^W$ plane
$M, C \in \mathbb{R}^{8 \times 8}$	Mass and Coriolis matrices
$G \in \mathbb{R}^8$	Gravity vector
$d \in \mathbb{R}^8$	Unknown (state-dependent) dynamics vectors
$\tau_p, \tau_q \in \mathbb{R}^3$	Generalized control inputs

unactuated cable-suspended payload dynamics; although [21] is applicable to underactuated dynamics, it models payload dynamics as a simple mass change of the quadrotor ignoring payload induced dynamic terms (e.g. rotor downwash). Further, the present work avoids any acceleration feedback which is required in [19], [21].

The rest of the paper is organised as follows: Sect. II describes the system dynamics and the control problem; Sect. III presents the proposed control scheme and its closed-loop stability analysis; Sect. IV illustrates the comparative experimental results while Sect. V presents concluding remarks.

The following notations are used in this paper: $\lambda_{\min}(\cdot)$ and $\|\cdot\|$ denote minimum eigenvalue and 2-norm of (\cdot) , respectively; I_n denotes identity matrix of dimension $n \times n$; $\text{diag}\{\cdot\}$ denotes diagonal matrix with elements $\{\cdot\}$; $(\cdot)^d$ denotes desired value of (\cdot) .

II. SYSTEM DYNAMICS AND PROBLEM FORMULATION

For the quadrotor system with suspended payload as in Fig. 2, the associated symbols and system parameters are defined in Table I. For system modelling, we take the following standard assumption:

Assumption 1: ([16], [17], [22], [23]) The cable connecting the payload and the quadrotor is attached to the center of mass of the quadrotor and it is massless, inelastic and always taut.

Under the above assumption and employing the Euler-Lagrangian formulation (cf. [24], [25]), the dynamic model of the composite system can be obtained as

$$M(q)\ddot{q} + C(q, \dot{q})\dot{q} + G(q) + d = [\tau_p^T \ \tau_q^T \ 0 \ 0]^T, \quad (1a)$$

$$\tau_p = R_B^W U, \quad (1b)$$

where $q(t) \triangleq [x(t), y(t), z(t), \phi(t), \theta(t), \psi(t), \alpha_x(t), \alpha_y(t)]$; $\tau_q(t) \triangleq [u_2(t), u_3(t), u_4(t)]$ is the control inputs for roll, pitch and yaw of the quadrotor; $\tau_p = R_B^W U$ is the generalized control input for quadrotor position in Earth-fixed frame, such that $U(t) \triangleq [0 \ 0 \ u_1(t)]^T$ being the force vector in body-fixed frame and R_B^W being the $Z - Y - X$ Euler angle rotation matrix describing the rotation from the body-fixed coordinate frame to the Earth-fixed frame [8]

$$R_B^W = \begin{bmatrix} c_\psi c_\theta & c_\psi s_\theta s_\phi - s_\psi c_\phi & c_\psi s_\theta c_\phi + s_\psi s_\phi \\ s_\psi c_\theta & s_\psi s_\theta s_\phi + c_\psi c_\phi & s_\psi s_\theta c_\phi - c_\psi s_\phi \\ -s_\eta & s_\phi c_\theta & c_\theta c_\phi \end{bmatrix}, \quad (2)$$

where $c(\cdot), s(\cdot)$ are abbreviations for $\cos(\cdot), \sin(\cdot)$ respectively. The term $d(\dot{q}, t)$ represents combined effects of external disturbances (e.g., wind, gust) and unmodelled state-dependent dynamics (e.g., low speed aerodynamic drag forces, rotor downwash, ground reaction disturbance). Following the standard properties of Euler-Lagrange systems (cf. [26, Ch. 6]) and of aerial vehicles (cf. [16], [17], [27, Ch. 3]), we state the following standard system properties:

Property 1: $\exists \bar{c}, \bar{g}, \bar{d}_0, \bar{d}_1 \in \mathbb{R}^+$ such that $\|C(q, \dot{q})\| \leq \bar{c}\|\dot{q}\|$, $\|G(q)\| \leq \bar{g}$ and $\|d(\dot{q}, t)\| \leq \bar{d}_0 + \bar{d}_1\|\dot{q}\|$.

Property 2: $M(q)$ is symmetric and uniformly positive definite. This implies that $\exists \mu_1, \mu_2 \in \mathbb{R}^+$ such that

$$0 < \mu_1 I_n \leq M(q) \leq \mu_2 I_n. \quad (3)$$

Consider the decomposition of M as $M = \hat{M} + \Delta M$, where \hat{M} and ΔM represent the nominal and perturbation terms of the mass matrix, respectively. The amount of uncertainty in the system is framed as an assumption below, which acts as a control challenge:

Assumption 2 (Uncertainty): Only the knowledge of \hat{M} and an upper bound for ΔM is available, while the terms C, G, d and their upper bounds $\bar{c}, \bar{g}, \bar{d}_0$ and \bar{d}_1 are unknown.

Remark 1 (Importance of state-dependent uncertainty): Property 1 highlights that the terms C and d create forces which directly depends on velocity; furthermore, motion in swing angles will excite motion in quadrotor via the coupling terms in inertia matrix M (cf. the structure in [24], [25]). Hence, uncertainty in these dynamic terms create state (i.e., velocity, acceleration)-dependent uncertainty. Crucially, it implies that these uncertainties, when unaddressed, will create unwanted motion in the system (cf. the system oscillations, drift etc. during the experiments later) leading to potential hazard.

For controller design, as well as for convenience of notation, let us rewrite system (1a) as

$$M(q)\ddot{q} + N(q, \dot{q})\dot{q} + d = [\tau^T \ 0 \ 0]^T \quad (4)$$

where

$$q \triangleq [q_a, q_u], \quad q_a = [x, y, z, \phi, \theta, \psi], \quad q_u = [\alpha_x, \alpha_y]$$

$$M \triangleq \begin{bmatrix} M_{aa} & M_{au} \\ M_{au}^T & M_{uu} \end{bmatrix}, \quad M_{aa} \in \mathbb{R}^{6 \times 6}, M_{au} \in \mathbb{R}^{6 \times 2}, \\ M_{uu} \in \mathbb{R}^{2 \times 2},$$

$$N \triangleq C\dot{q} + G = [N_a, N_u], \quad N_a \in \mathbb{R}^6, N_u \in \mathbb{R}^2,$$

$$d \triangleq [d_a, d_u], \quad d_a \in \mathbb{R}^6, d_u \in \mathbb{R}^2, \tau \triangleq [\tau_p, \tau_q].$$

Using these decomposed representations of M, N and d , the system dynamics (4) can further be represented as

$$\ddot{q}_u = -M_{uu}^{-1}M_{au}^T\ddot{q}_a + h_u, \quad (5a)$$

$$\ddot{q}_a = M_s^{-1}\tau + h_a, \quad (5b)$$

where $h_u \triangleq M_{uu}^{-1}(N_u + d_u)$,

$$h_a \triangleq M_s^{-1}(N_a + d_a - M_{au}M_{uu}^{-1}(N_u + d_u)),$$

$$M_s \triangleq M_{aa} - M_{au}M_{uu}^{-1}M_{au}^T.$$

Control Objective: Under Assumptions 1-2 and Properties 1-2, to design an adaptive controller to maintain the quadrotor at a desired fixed location (x^d, y^d, z^d) , while stabilizing the attitude and payload swing angles (i.e., $\phi^d = \theta^d = \psi^d = \alpha_x^d = \alpha_y^d = 0$).

The following section solves this control problem along with detailed analysis.

III. PROPOSED CONTROLLER DESIGN AND ANALYSIS

Let us define tracking error $e_a \triangleq q_a - q_a^d$ and an auxiliary error variable r as

$$r \triangleq \Upsilon_a \dot{e}_a + \Gamma_a e_a + \Upsilon_u \dot{q}_u + \Gamma_u q_u, \quad (6)$$

where $\Upsilon_a, \Gamma_a \in \mathbb{R}^{6 \times 6}$ are positive definite and $\Upsilon_u, \Gamma_u \in \mathbb{R}^{6 \times 2}$ are full rank user-defined matrices, respectively.

Using (5a) and (5b), the time derivative of (6) yields

$$\begin{aligned} \dot{r} &= \Upsilon_a \ddot{q}_a + \Gamma_a \dot{e}_a + \Upsilon_u \ddot{q}_u + \Gamma_u \dot{q}_u \\ &= (\Upsilon_a - \Upsilon_u M_{uu}^{-1} M_{au}^T)(M_s^{-1}\tau + h_a) + \Upsilon_u h_u \\ &\quad + \Gamma_a \dot{e}_a + \Gamma_u \dot{q}_u \\ &= b\tau + \varphi + S_r, \end{aligned} \quad (7)$$

where $b \triangleq (\Upsilon_a - \Upsilon_u M_{uu}^{-1} M_{au}^T)M_s^{-1}$
 $\varphi \triangleq (\Upsilon_a - \Upsilon_u M_{uu}^{-1} M_{au}^T)h_a + \Upsilon_u h_u$
 $S_r \triangleq \Gamma_a \dot{e}_a + \Gamma_u \dot{q}_u$.

The control law is designed as

$$\tau = \hat{b}^{-1}(-\Lambda r - S_r - \Delta\tau), \quad \Delta\tau = \rho \frac{r}{\|r\|}, \quad (8)$$

where $\Lambda \in \mathbb{R}^{6 \times 6}$ is user-defined positive definite matrix; ρ is the adaptive gain for tackling uncertainties and will be discussed later. Finally, \hat{b} is the nominal value of b which satisfies the condition

$$\|b\hat{b}^{-1} - I_6\| \leq E < 1. \quad (9)$$

Remark 2: The value of E can be calculated based on \hat{M} and the upper bound of ΔM (cf. Assumption 2): such condition is quite standard in robotics literature [26]. Substituting (8) into (7) yields

$$\dot{r} = -\Lambda r - \Delta\tau + \sigma - (b\hat{b}^{-1} - I_6)\Delta\tau, \quad (10)$$

where $\sigma \triangleq \varphi - (b\hat{b}^{-1} - I_6)(\Lambda r + S_r)$. From *Properties 1* and *2*, one can verify

$$\|N\| \leq \|C\| \|\dot{q}\| + \|G\| \leq \bar{c} \|\dot{q}\|^2 + \bar{g}. \quad (11)$$

Let us define $\xi \triangleq [e^T \ \dot{e}^T]^T = [e_a^T \ q_u^T \ \dot{e}_a^T \ \dot{q}_u^T]^T$. Then, using the fact $\dot{e} = \dot{q}$ (as $\dot{q}^d = 0$), Property 1, and the inequalities $\|N_u\| \leq \|N\|, \|N_a\| \leq \|N\|, \|d_u\| \leq \|d\|, \|d_a\| \leq \|d\|, \|e_a\| \leq \|\xi\|, \|q_u\| \leq \|\xi\|, \|\dot{e}_a\| \leq \|\xi\|, \|\dot{q}_u\| \leq \|\xi\|$ in (5), the following bound can be obtained:

$$\begin{aligned} \|\sigma\| &= \|\varphi - (b\hat{b}^{-1} - I_6)(\Lambda r + S_r)\| \\ &\leq \|\varphi\| + E(\|\Lambda\| \|r\| + \|S_r\|), \\ &\leq \kappa_0^* + \kappa_1^* \|\xi\| + \kappa_2^* \|\xi\|^2, \end{aligned} \quad (12)$$

with $\kappa_0^* \triangleq a\bar{g} + \|\Upsilon_u\| \|M_{uu}^{-1}\| (\bar{g} + \bar{d}) + a_1$,
 $\kappa_1^* \triangleq E(\|\Gamma_a\| + \|\Gamma_u\|) + a_2, \kappa_2^* \triangleq a\bar{c} + \|\Upsilon_u\| \|M_{uu}^{-1}\| \bar{c}$,
 $a \triangleq \|(\Upsilon_a - \Upsilon_u M_{uu}^{-1} M_{au})\| (\|M_s^{-1}\| + \|M_{au} M_{uu}^{-1}\|)$,
 $a_1 \triangleq \|(\Upsilon_a - \Upsilon_u M_{uu}^{-1} M_{au})\| \|M_s^{-1}\| (1 + \|M_{au} M_{uu}^{-1}\|) \bar{d}$,
 $a_2 \triangleq E\|\Lambda\| (\|\Upsilon_a\| + \|\Gamma_a\| + \|\Upsilon_u\| + \|\Gamma_u\|)$

where the scalars $\kappa_i^* \in \mathbb{R}^+, i = 0, 1, 2$ are *unknown* as per Assumption 2.

Using (5a)-(5b), the payload swing dynamics can be represented as

$$\begin{aligned} \ddot{q}_u &= -M_{uu}^{-1}M_{au}^T\ddot{q}_a + h_u \\ &= -M_{uu}^{-1}M_{au}^T(M_s^{-1}\tau + h_a) + h_u. \end{aligned} \quad (13)$$

Substituting (8) into (13) yields

$$\begin{aligned} \dot{\chi}_1 &= \chi_2 \\ \dot{\chi}_2 &= -\varpi v - \varphi_1, \end{aligned} \quad (14)$$

where $\chi_1 \triangleq q_u, \chi_2 \triangleq \dot{q}_u, \varphi_1 \triangleq (M_{uu}^{-1}M_{au}^T h_a + h_u), v \triangleq (-\Lambda r - S_r - \Delta\tau), \varpi \triangleq (M_{uu}^{-1}M_{au}^T M_s^{-1})\hat{b}^{-1}$. One can design a constant full-rank matrix $H \in \mathbb{R}^{2 \times 6}$ such that

$$K_1 \triangleq H\Lambda\Gamma_u, \quad K_2 \triangleq H\Lambda\Upsilon_u \quad (15)$$

are positive definite matrices. Adding and subtracting Hv to (14) yields

$$\begin{aligned} \dot{\chi}_1 &= \chi_2 \\ \dot{\chi}_2 &= -K_1\chi_1 - K_2\chi_2 + \varpi\Delta\tau + \varphi_2, \end{aligned} \quad (16)$$

where $\varphi_2 \triangleq gS_r + (H + \varpi)\Lambda r - \varphi_1 - H\Lambda(\Upsilon_a \dot{e}_a + \Gamma_a e_a)$ acts as *uncertainty in the payload swing dynamics*. Taking $\chi \triangleq [\chi_1^T \ \chi_2^T]^T, A \triangleq \begin{bmatrix} 0 & I_2 \\ -K_1 & -K_2 \end{bmatrix}$ and $B \triangleq [0 \ I_2]^T$, one has from (16)

$$\dot{\chi} = A\chi + B(\varpi\Delta\tau + \varphi_2) \quad (17)$$

where positive definiteness of K_1, K_2 guarantees that A is Hurwitz. From *Properties 1-2*, the following holds

$$\|\varphi_2\| \|PB\| \leq (\kappa_0^{**} + \kappa_1^{**}\|\xi\| + \kappa_2^{**}\|\xi\|^2), \quad (18)$$

where $\kappa_i^{**} \in \mathbb{R}^+, i = 0, 1, 2$ are unknown scalars whose expressions follow from similar steps as (12); $P > 0$ is the solution to the Lyapunov equation $A^T P + PA = -Q$ for some positive definite matrix Q .

Observing the upper bounds structures of $\|\sigma\|$ and $\|\varphi_2\|$ in (12) and (18) respectively, we design ρ in (8) as

$$\rho = \frac{1}{(1-E)} (\hat{\kappa}_0 + \hat{\kappa}_1 \|\xi\| + \hat{\kappa}_2 \|\xi\|^2 + \gamma), \quad (19)$$

with adaptive laws ($i = 0, 1, 2$)

$$\dot{\hat{\kappa}}_i = (\|r\| + \|\chi\|)\|\xi\|^i - \zeta_i \hat{\kappa}_i \beta \|\chi\| \|\xi\|^i, \quad (20a)$$

$$\dot{\gamma} = -\gamma \{ \gamma_0 + \gamma_1 (\|\xi\|^5 - \|\xi\|^4) + \gamma_2 (\|\chi\| + \|\xi\|) \} + \gamma_0 (\|r\| + \|\chi\|) + \gamma_0 \nu, \quad (20b)$$

$$\text{initial conditions } \hat{\kappa}_i(0) > 0, \gamma(0) > \nu, \quad (20c)$$

$$\text{and } \eta_i, \zeta_i, \beta, \gamma_0, \gamma_1, \gamma_2, \nu \in \mathbb{R}^+, \quad (20d)$$

satisfying the following inequalities

$$\gamma_2 \geq \gamma_1, \beta > 1 + (E_1/(1 - E)), \quad (20e)$$

with E_1 being a constant satisfying $\|PBg\| \leq E_1$, and derived from the known upper bound of ΔM in Assumption 2 In (20), $\hat{\kappa}_i$ is the estimate of $\bar{\kappa}_i^* \triangleq \max\{\kappa_i^*, \kappa_i^{**}\}$, $i = 0, 1, 2$; γ is an auxiliary gain which helps in closed-loop system stabilization (cf. discussion before (32)). It can be verified that the design $\gamma_0, \gamma_1, \gamma_2 \in \mathbb{R}^+$ with $\gamma_2 \geq \gamma_1$ makes the term ' $\gamma_0 + \gamma_1 (\|\xi\|^5 - \|\xi\|^4) + \gamma_2 (\|\chi\| + \|\xi\|)$ ' in (20b) positive for all χ, ξ .

IV. EXPERIMENTAL RESULTS AND ANALYSIS

The proposed controller is tested on a quadrotor setup (Q-450 frame with Turnigy SK3-2826 brushless motors, weighing ~ 1.5 kg), with a payload (~ 0.2 kg) suspended from its center. Raspberry Pi-4 is used as a processing unit and joystick potentiometer is used to measure swing angles of payload (cf. [25] for such arrangement). Optitrack motion capture system (at 120 fps) and IMU were used to obtain system pose and state-derivatives were obtained via fusing these sensor data for the necessary feedback.

To verify the effectiveness of the proposed control law, we compare it with the adaptive method [16]. The following control design parameters are selected for the proposed controller during the experimentation: $\Upsilon_a = \text{diag}\{1, 1, 3, 2, 2, 2\}$, $\Gamma_a = \text{diag}\{1, 1, 2, 4, 4, 4\}$, $\Upsilon_u = \begin{bmatrix} 0.02 & 0 & 0 & 0 & 0 & 0 \\ 0 & 0.02 & 0 & 0 & 0 & 0 \end{bmatrix}^T$, $\Gamma_u = 2.5\Upsilon_u$, $\hat{b} = \text{diag}\{1.5, 1.5, 1.5, 0.02, 0.02, 0.04\}$, $E = 0.3$, $\hat{\kappa}_0(0) = \hat{\kappa}_1(0) = \hat{\kappa}_2(0) = 0.01$, $\gamma(0) = 0.1$, $\Lambda = \text{diag}\{1.0, 1.0, 1.2, 0.5, 0.5, 0.2\}$, $\eta_0 = 2, \eta_1 = 3, \eta_2 = 1, \zeta_0 = 1, \zeta_1 = 2, \zeta_2 = 1, \beta = 3, \gamma_0 = 2, \gamma_1 = 1, \gamma_2 = 2, \nu = 0.001, \epsilon = 0.1$. For the adaptive controller [16], the various control parameters are selected as in [16].

A. Experimental Scenario

During payload delivery operation via cable-suspended mode, human interacts closely with the quadrotor while attaching or detaching the payload; during such interaction, payload swing can happen and if not properly stabilized, such swings can cause safety hazard. We have created an experimental scenario in an attempt to emulate such phenomenon (cf. Fig. 3): in this scenario, the quadrotor hovers at a given position ($x^d = y^d = 0, z^d = 1\text{m}$) and, suddenly, the payload is pushed by a stick at $t = 2\text{s}$ (approx.) to create swing angles. As mentioned before in Remark 2, the motion in swing angles create state-dependent uncertainty. Therefore, such an experimental scenario tests the capability

of a controller to negotiate state-dependent disturbances. Additionally, a fan is used to introduce wind disturbance.

B. Results and Discussion

The performances of the controllers are compared via Figs. 4-6 and via Table II. The red marked zones in Figs. 6-6 highlight the oscillations caused by the stick. It can be observed that the proposed controller could successfully damp the swing angle oscillations even with higher initial overshoots compared to the other controllers. Whereas, in absence of any measure to deal with state-dependent uncertainty, [16] fails to damp the oscillations in swing angles leading to sustained oscillations and drift in the quadrotor positions (cf. Fig. 4 after $t = 2\text{s}$). This can cause hazard to human operator.

TABLE II: Root-Mean-Squared (RMS) error comparison

Controller	Position error (m)			Attitude error (deg)		
	x	y	z	ϕ	θ	ψ
Proposed	0.02	0.06	0.02	3.5	3.1	3.8
Adaptive [16]	0.08	0.08	0.12	14.8	13.05	6.6
Controller	Swing angle error (deg)					
	α_x	α_y				
Proposed	8.5	6.9				
Adaptive [16]	15.1	15.9				

V. CONCLUSION

Having in mind the human-quadrotor interaction during clasping and unclasping of a cable-suspended payload, this work has proposed and analyzed a suitable adaptive anti-swing controller. The suitability of the solution comes from the fact that, contrary to the state-of-the-art, the controller was designed to handle unknown state-dependent uncertainty in such dynamics. Experimental studies showed that the proposed control framework was safer and could significantly damp the unwanted payload swings compared to the state of the art.

APPENDIX

PROOF OF THEOREM 1

From the adaptive law (20b) and initial condition (20c), it can be verified that $\exists \underline{\gamma}, \gamma \in \mathbb{R}^+$ such that

$$0 < \underline{\gamma} \leq \gamma(t) \leq \bar{\gamma} \quad \forall t \geq 0. \quad (21)$$

Stability is analyzed via the Lyapunov function:

$$V = \frac{1}{2} r^T r + \frac{1}{2} \chi^T P \chi + \frac{1}{2} \sum_{i=0}^2 (\hat{\kappa}_i - \bar{\kappa}_i^*)^2 + \frac{\gamma}{\underline{\gamma}}, \quad (22)$$

where $\bar{\kappa}_i^* = \max\{\kappa_i^*, \kappa_i^{**}\}$.

Using (8), (12) and (19), from (7) we have

$$\begin{aligned} r^T \dot{r} &= r^T (-\Lambda r - \Delta \tau + \sigma - (b\hat{b}^{-1} - I_6) \Delta \tau) \\ &\leq -r^T \Lambda r - (1 - E) \rho \|r\| + \sum_{i=0}^2 \kappa_i^* \|\xi\|^i \|r\| \\ &\leq -r^T \Lambda r - \sum_{i=0}^2 \hat{\kappa}_i \|\xi\|^i \|r\| + \bar{\kappa}_i^* \|\xi\|^i \|r\|. \end{aligned} \quad (23)$$

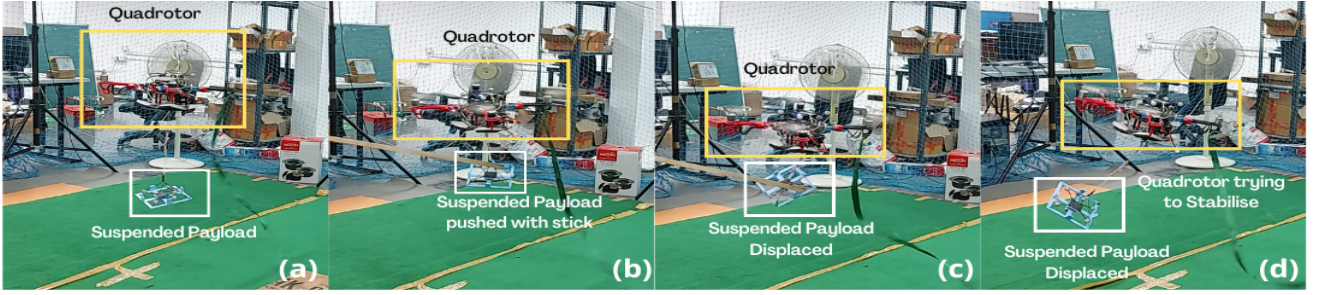


Fig. 3: Snapshots from experimental scenario with the proposed controller: a) quadrotor takes off with the suspended payload; b) payload is pushed at $t = 2s$ with a stick c) payload is displaced d) quadrotor tries to stabilise itself.

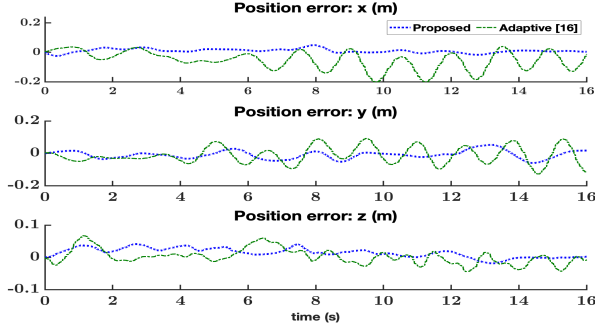


Fig. 4: Quadrotor position tracking error.

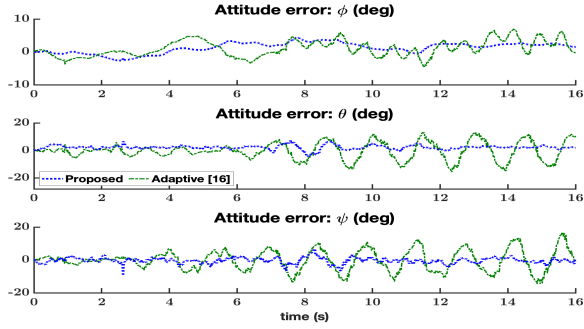


Fig. 5: Quadrotor attitude tracking error.

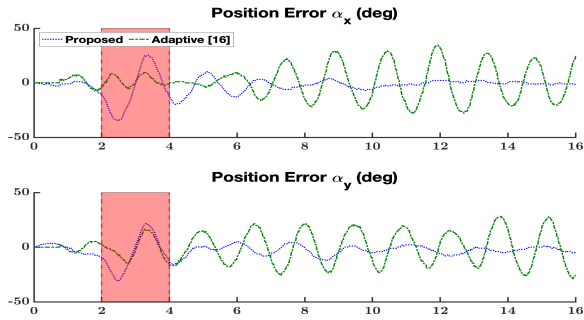


Fig. 6: Stabilization error in payload swing angles α_x and α_y .

where we have used the fact that $\gamma > 0$ from (21). Further,

using (17) and (18) we have

$$\begin{aligned} \frac{1}{2} \frac{d}{dt} \chi^T P \chi &= -\frac{1}{2} \chi^T Q \chi + \chi^T P B (\omega \Delta \tau + \varphi_2) \\ &\leq -\frac{1}{2} \chi^T Q \chi + \rho E_1 \|\chi\| + \|\varphi_2\| \|PB\| \|\chi\| \\ &\leq -\frac{1}{2} \chi^T Q \chi + \sum_{i=0}^2 (\bar{\kappa}_i^* \|\xi\|^i + \frac{E_1 (\hat{\kappa}_i \|\xi\|^i + \gamma)}{1-E}) \|\chi\|. \end{aligned} \quad (24)$$

Using the adaptive laws (20a), (20b), and (21) we have

$$\begin{aligned} (\hat{\kappa}_i - \bar{\kappa}_i^*) \dot{\hat{\kappa}}_i &= \hat{\kappa}_i (\|r\| + \|\chi\|) \|\xi\|^i - \beta \hat{\kappa}_i^2 \|\chi\| \|\xi\|^i \\ &\quad - \bar{\kappa}_i^* (\|r\| + \|\chi\|) \|\xi\|^i + \beta \hat{\kappa}_i \bar{\kappa}_i^* \|\chi\| \|\xi\|^i, \quad (25) \\ \dot{\underline{\gamma}} &= -\frac{\underline{\gamma}}{\underline{\gamma}} (1 + \gamma_1 \|\xi\|^4) + \frac{\nu}{\underline{\gamma}} \leq -\gamma_1 \|\xi\|^4 + (\nu/\underline{\gamma}), \quad (26) \end{aligned}$$

where we have used the fact that $\gamma \geq \underline{\gamma}$ from (21). Using (23)-(26), the time derivative of the Lyapunov function (22) turns out to satisfy

$$\begin{aligned} \dot{V} &\leq -\delta_m (\|r\|^2 + \|\chi\|^2) - \gamma_1 \|\xi\|^4 + (\nu/\underline{\gamma}) + c\gamma \|\chi\| \\ &\quad + \sum_{i=0}^2 (c\hat{\kappa}_i - \beta \hat{\kappa}_i^2 + \beta \hat{\kappa}_i \bar{\kappa}_i^*) \|\xi\|^i \|\chi\|, \quad (27) \end{aligned}$$

where $\delta_m \triangleq \min\{\lambda_{\min}(\Lambda), (1/2)\lambda_{\min}(Q)\}$ and $c \triangleq 1 + \frac{E_1}{1-E}$. From (22), the definition of V yields

$$V \leq \delta_M (\|r\|^2 + \|\chi\|^2) + \sum_{i=0}^2 (\hat{\kappa}_i^2 + \bar{\kappa}_i^{*2}) + \frac{\bar{\gamma}}{\underline{\gamma}}, \quad (28)$$

where $\delta_M \triangleq \max\{1, \|P\|\}$. Defining $\Omega \triangleq (\delta_m/\delta_M)$, (27) is further simplified using (28) as

$$\begin{aligned} \dot{V} &\leq -\Omega V - \gamma_1 \|\xi\|^4 + (\nu/\underline{\gamma}) + (\Omega\bar{\gamma})/\underline{\gamma} + c\gamma \|\chi\| \\ &\quad + \sum_{i=0}^2 (c\hat{\kappa}_i - \beta \hat{\kappa}_i^2 + \beta \hat{\kappa}_i \bar{\kappa}_i^*) \|\xi\|^i \|\chi\| + \Omega (\hat{\kappa}_i^2 + \bar{\kappa}_i^*)^2. \quad (29) \end{aligned}$$

Since $\beta > 1$ by design (20d), it is always possible to split β as $\beta = \beta_1 + \beta_2 + \beta_3$ where $\beta_i > 0$, $i = 1, 2, 3$. Then, the

following simplification can be made

$$\begin{aligned}
& -\beta\hat{\kappa}_i^2 + c\hat{\kappa}_i + \beta\hat{\kappa}_i\bar{\kappa}_i^* = -\beta_1\hat{\kappa}_i^2 - \beta_2 \left\{ \left(\hat{\kappa}_i - \frac{c}{2\beta_2} \right)^2 - \frac{c^2}{4\beta_2^2} \right\} \\
& \quad - \beta_3 \left\{ \left(\hat{\kappa}_i - \frac{\beta\bar{\kappa}_i^*}{2\beta_3} \right)^2 - \frac{(\beta\bar{\kappa}_i^*)^2}{4\beta_3^2} \right\} \\
& \leq -\beta_1\hat{\kappa}_i^2 + \frac{c^2}{4\beta_2} + \frac{(\beta\bar{\kappa}_i^*)^2}{4\beta_3}. \tag{30}
\end{aligned}$$

Using (30), the inequality (29) becomes

$$\dot{V} \leq -\Omega V - \sum_{i=0}^2 (\beta_1 \|\chi\|^{(i+1)} - \Omega) \hat{\kappa}_i^2 + f(\|\xi\|), \tag{31}$$

where $f(\|\xi\|) \triangleq -\gamma_1 \|\xi\|^4 + \varsigma_3 \|\xi\|^3 + \varsigma_2 \|\xi\|^2 + \varsigma_1 \|\xi\| + \varsigma_0$,

$$\varsigma_3 \triangleq c^2/(4\beta_2) + (\beta\bar{\kappa}_2^*)^2/(4\beta_3),$$

$$\varsigma_2 \triangleq \frac{c^2}{4\beta_2} + \frac{(\beta\bar{\kappa}_1^*)^2}{4\beta_3}, \varsigma_1 \triangleq \frac{c^2}{2\beta_2} + \frac{(\beta\bar{\kappa}_0^*)^2}{4\beta_3} + c\bar{\gamma},$$

$$\varsigma_0 \triangleq \Omega(\bar{\kappa}_0^{*2} + \bar{\kappa}_1^{*2} + \bar{\kappa}_2^{*2}) + (\nu/\underline{\gamma}) + (\Omega\bar{\gamma})/\underline{\gamma}.$$

Bolzano's Theorem and Descartes' rule of sign change imply that the polynomial f has finite positive real roots; let $\iota \in \mathbb{R}^+$ be the maximum positive real root of f . Since the coefficient of the highest degree of f is negative as $\gamma_1 \in \mathbb{R}^+$, $f(\|\xi\|) \leq 0$ when $\|\xi\| \geq \iota$. This was possible owing to the negative fourth degree term $-\gamma_1 \|\xi\|^4$ contributed by $\dot{\gamma}$. Define $\iota_1 \triangleq \max\{(\Omega/\beta_1), (\Omega/\beta_1)^{\frac{2}{3}}, (\Omega/\beta_1)^{\frac{1}{3}}\}$. Hence, from (31), $\dot{V} \leq -\Omega V$ when

$$\begin{aligned}
& \min \{ \|\chi\|, \|\xi\| \} \geq \max \{ \iota, \iota_1 \} \\
& \Rightarrow \|\chi\| \geq \max \{ \iota, \iota_1 \}, \tag{32}
\end{aligned}$$

implying that the closed-loop system is UUB and $r, q_u, \dot{q}_u, \hat{\kappa}_i, \gamma$ remain bounded; again, boundedness of r, q_u, \dot{q}_u ensures that e_a, \dot{e}_a are bounded from (6).

REFERENCES

- [1] P. Pereira, J. Cortés, and D. V. Dimarogonas, "Aerial slung-load position tracking under unknown wind forces," *IEEE Trans. Autom. Control*, vol. 66, no. 9, pp. 3952–3968, 2020.
- [2] D. Invernizzi, M. Lovera, and L. Zaccarian, "Integral ISS-based cascade stabilization for vectored-thrust UAVs," *IEEE Control Systems Letters*, vol. 4, no. 1, pp. 43–48, 2019.
- [3] L. Fusini, T. I. Fossen, and T. A. Johansen, "Nonlinear observers for GNSS-and camera-aided inertial navigation of a fixed-wing UAV," *IEEE Trans. Control Syst. Technol.*, vol. 26, no. 5, pp. 1884–1891, 2018.
- [4] K. Sreenath, N. Michael, and V. Kumar, "Trajectory generation and control of a quadrotor with a cable-suspended load - a differentially-flat hybrid system," in *2013 IEEE Int. Conf. Robot. Autom.*, 2013, pp. 4888–4895.
- [5] S. Tang and V. Kumar, "Mixed integer quadratic program trajectory generation for a quadrotor with a cable-suspended payload," pp. 2216–2222, 2015.
- [6] S. Yang and B. Xian, "Energy-based nonlinear adaptive control design for the quadrotor uav system with a suspended payload," *IEEE Trans. Ind. Electron.*, vol. 67, no. 3, pp. 2054–2064, 2020.
- [7] B. Xian and S. Yang, "Robust tracking control of a quadrotor unmanned aerial vehicle-suspended payload system," *IEEE/ASME Trans. Mechatron.*, vol. 26, no. 5, pp. 2653–2663, 2021.
- [8] D. Mellinger and V. Kumar, "Minimum snap trajectory generation and control for quadrotors," in *IEEE Int. Conf. Robot. Autom.* IEEE, 2011, pp. 2520–2525.
- [9] V. N. Sankaranarayanan, S. Roy, and S. Baldi, "Aerial transportation of unknown payloads: Adaptive path tracking for quadrotors," in *IEEE/RSJ Int. Conf. Intell. Robots Syst. (IROS)*, 2020, pp. 7710–7715.
- [10] B. J. Bialy, J. Klotz, K. Brink, and W. E. Dixon, "Lyapunov-based robust adaptive control of a quadrotor UAV in the presence of modeling uncertainties," *ACC*, pp. 13–18, 2013.
- [11] G. Loianno, V. Spurny, J. Thomas, T. Baca, D. Thakur, D. Hert, R. Penicka, T. Krajnik, A. Zhou, A. Cho *et al.*, "Localization, grasping, and transportation of magnetic objects by a team of mavs in challenging desert-like environments," *IEEE Rob. Autom. Lett.*, vol. 3, no. 3, pp. 1576–1583, 2018.
- [12] L. Qian and H. H. Liu, "Path-following control of a quadrotor uav with a cable-suspended payload under wind disturbances," *IEEE Trans. Ind. Electron.*, vol. 67, no. 3, pp. 2021–2029, 2019.
- [13] D. Cabecinhas, R. Cunha, and C. Silvestre, "A trajectory tracking control law for a quadrotor with slung load," *Automatica*, vol. 106, pp. 384–389, 2019.
- [14] H. Hua, Y. Fang, X. Zhang, and C. Qian, "A new nonlinear control strategy embedded with reinforcement learning for a multirotor transporting a suspended payload," *IEEE/ASME Trans. Mechatron.*, vol. 27, no. 2, pp. 1174–1184, 2022.
- [15] G. Yu, W. Xie, D. Cabecinhas, R. Cunha, and C. Silvestre, "Adaptive control with unknown mass estimation for a quadrotor-slung-load system," *ISA Trans.*, vol. 133, pp. 412–423, 2023.
- [16] X. Liang, Y. Fang, N. Sun, H. Lin, and X. Zhao, "Adaptive nonlinear hierarchical control for a rotorcraft transporting a cable-suspended payload," *IEEE Trans. Syst. Man Cybern.: Syst.*, vol. 51, no. 7, pp. 4171–4182, 2021.
- [17] Z.-Y. Lv, S. Li, Y. Wu, and Q.-G. Wang, "Adaptive control for a quadrotor transporting a cable-suspended payload with unknown mass in the presence of rotor downwash," *IEEE Trans. Veh. Technol.*, vol. 70, no. 9, pp. 8505–8518, 2021.
- [18] X. Liang, Y. Fang, N. Sun, and H. Lin, "A novel energy-coupling-based hierarchical control approach for unmanned quadrotor transportation systems," *IEEE/ASME Trans. Mechatron.*, vol. 24, no. 1, pp. 248–259, 2019.
- [19] S. Dantu, R. D. Yadav, S. Roy, J. Lee, and S. Baldi, "Adaptive artificial time delay control for quadrotors under state-dependent unknown dynamics," in *2022 IEEE Int. Conf. Robot. Biomim.* IEEE, 2022, pp. 1092–1097.
- [20] V. N. Sankaranarayanan, R. D. Yadav, R. K. Swayampakula, S. Ganguly, and S. Roy, "Robustifying payload carrying operations for quadrotors under time-varying state constraints and uncertainty," *IEEE Rob. Autom. Lett.*, vol. 7, no. 2, pp. 4885–4892, 2022.
- [21] S. Roy, S. Baldi, P. Li, and V. N. Sankaranarayanan, "Artificial-delay adaptive control for underactuated euler-lagrange robotics," *IEEE/ASME Trans. Mechatron.*, vol. 26, no. 6, pp. 3064–3075, 2021.
- [22] X. Liang, Y. Fang, N. Sun, H. Lin, and X. Zhao, "Adaptive nonlinear hierarchical control for a rotorcraft transporting a cable-suspended payload," *IEEE Trans. Syst. Man Cybern.: Syst.*, vol. 51, no. 7, pp. 4171–4182, 2019.
- [23] S. Yang and B. Xian, "Energy-based nonlinear adaptive control design for the quadrotor uav system with a suspended payload," *IEEE Trans. Ind. Electron.*, vol. 67, no. 3, pp. 2054–2064, 2019.
- [24] M. E. Guerrero, D. Mercado, R. Lozano, and C. García, "Passivity based control for a quadrotor uav transporting a cable-suspended payload with minimum swing," in *2015 54th IEEE Conf. Decis. Control.* IEEE, 2015, pp. 6718–6723.
- [25] M. E. Guerrero-Sánchez, D. A. Mercado-Ravell, R. Lozano, and C. D. García-Beltrán, "Swing-attenuation for a quadrotor transporting a cable-suspended payload," *ISA Trans.*, vol. 68, pp. 433–449, 2017.
- [26] M. W. Spong, S. Hutchinson, and M. Vidyasagar, *Robot modeling and control.* Wiley New York, 2006.
- [27] R. W. Beard and T. W. McLain, *Small unmanned aircraft: Theory and practice.* Princeton University Press, 2012.